Molecular Microbiology (2006) **59**(5), 1369–1379
doi:10.1111/j.1365-2958.2005.05024.x
First published online 20 January 2006

CelTOS, a novel malarial protein that mediates transmission to mosquito and vertebrate hosts

Tohru Kariu,[1†§] Tomoko Ishino,[1,2§] Kazuhiko Yano,[1‡] Yasuo Chinzei[1,2] and Masao Yuda[1,2*]
[1]*Mie University, School of Medicine, 2–174 Edobashi, Tsu, Mie 514-0001, Japan.*
[2]*CREST, Japan Science and Technology Agency, Kawaguchi, Saitama, Japan.*

Summary

The malarial parasite has two hosts in its life cycle, a vertebrate and a mosquito. We report here that malarial invasion into these hosts is mediated by a protein, designated cell-traversal protein for ookinetes and sporozoites (CelTOS), which is localized to micronemes that are organelles for parasite invasive motility. Targeted disruption of the CelTOS gene in *Plasmodium berghei* reduced parasite infectivity in the mosquito host approximately 200-fold. The disruption also reduced the sporozoite infectivity in the liver and almost abolished its cell-passage ability. Liver infectivity was restored in Kupffer cell-depleted rats, indicating that CelTOS is necessary for sporozoite passage from the circulatory system to hepatocytes through the liver sinusoidal cell layer. Electron microscopic analysis revealed that *celtos*-disrupted ookinetes invade the midgut epithelial cell by rupturing the cell membrane, but then fail to cross the cell, indicating that CelTOS is necessary for migration through the cytoplasm. These results suggest that conserved cell-passage mechanisms are used by both sporozoites and ookinetes to breach host cellular barriers. Elucidation of these mechanisms might lead to novel antimalarial strategies to block parasite's transmission.

Introduction

The malarial parasite infects both mammalian and mosquito hosts during its complex life cycle. When the parasite changes hosts, it develops motile stages that can invade the target organ in the new host, heading for the site where it can proliferate to the next motile stage. In this migration, the parasite encounters host cell barriers that hamper its advance. To circumvent these barriers and penetrate the organ, the parasite invades and traverses host cells. Cell-traversal ability is thus essential for the parasite to establish an infection in a new host.

After a female mosquito ingests an infective blood meal, sexual-stage parasites are fertilized in the mosquito midgut lumen and develop into motile ookinetes. The ookinete invades the mosquito midgut epithelium and moves to the midgut basement membrane, on which it forms an oocyst and transforms into thousands of sporozoites, the salivary gland-invasive form. Malarial ookinetes traverse a single epithelial cell or additionally some neighbouring epithelial cells before they arrive at the basal lamina, indicating that cell-traversal ability is essential for the ookinete to establish infection in the mosquito vector. A recently proposed model of ookinete infection of the midgut (Zieler and Dvorak, 2000; Han and Barillas-Mury, 2002) suggests that epithelial cells invaded by ookinetes soon die and are then ejected from the midgut wall, which exposes the parasites to the danger of being removed from the epithelium with the damaged cell and requires the ookinetes to cross this layer in a limited time. Furthermore, during this midgut invasion, many ookinetes are killed by the insect defence system, and the number of malarial parasites is greatly reduced (Blandin *et al*., 2004). Thus, prompt passage through the epithelial cell is critical for the parasite's successful infection of the mosquito vector.

Malarial transmission to the mammalian host is accomplished by sporozoite infection of the hepatocyte, in which it forms a parasitophorous vacuole and develops into thousands of erythrocyte-invasive forms. Sporozoites gathered in the mosquito salivary glands are injected into the mammalian host by a mosquito bite. The sporozoites enter the blood circulation and are transported to the liver sinusoid. There they leave the circulation by crossing the liver sinusoidal layer, the boundary between the circulation and hepatocytes. Ultrastructural studies indicate that Kupffer cells, which are hepatic macrophages and major components of the sinusoidal cell layer, are routes of this crossing, based on the observation that sporozoites remain in Kupffer cells shortly after intravenous inoculation (Meis *et al*., 1983). We reported that cell-passage ability is essential for the sporozoite to cross this 'blood-

Accepted 2 December, 2005. *For correspondence. E-mail m-yuda@doc.medic.mie-u.ac.jp; Tel. (+81) 592315013; Fax (+81) 592315215. Present addresses: †Sojo University, School of Pharmacological Sciences, 4-22-1 Ikeda, Kumamoto-shi, Kumamoto 860-0082, Japan. ‡Research Institute, International Medical Center of Japan, 1-21-1 Toyama, Shinjuku-ku, Tokyo 162-8655, Japan. §These authors contributed equally to this work.

hepatocytic barrier' and that novel microneme proteins, named sporozoite micronemal protein essential for cell traversal (SPECT) and SPECT2, are necessary for this crossing (Ishino *et al*., 2004; 2005; Kaiser *et al*., 2004).

Motile stages of the malarial parasite have no locomotory organelles, such as flagella or cilia. Instead, their motility requires substrates and is achieved by highly developed cytoplasmic secretory organelles, called micronemes. The motile stages secrete the micronemal contents from an apical pore and translocate them along the cell surface (Menard, 2001). This backward movement, which is powered by an actomyosin motor of the parasite (Dobrowolski and Sibley, 1996), creates motility by gaining a foothold outside. In the sporozoite stage, thrombospondin-related anonymous protein (TRAP), a microneme protein with a single transmembrane domain, has a pivotal role in transmitting the driving force outside the plasma membrane (Sultan *et al*., 1997). Linked with the actomyosin motor in the cytoplasm (Kappe *et al*., 1999; Buscaglia *et al*., 2003; Jewett and Sibley, 2003), TRAP moves backwards along the parasite plasma membrane and generates surface movement. Similar driving mechanisms might be used by the ookinete to pass through the midgut epithelial cells, because a micronemal protein paralogous to TRAP has an essential role in this process (Yuda *et al*., 1999a; Dessens *et al*., 2000). It is now believed that cognate driving machinery involving TRAP-family proteins is widely used by apicomplexan parasites to invade host cells (Spano *et al*., 1998).

To search for genes involved in parasite invasive motility, we performed a comparative analysis of expressed sequence tag (EST) databases of two motile stages, salivary gland sporozoites and ookinetes, of the rodent malarial parasite *Plasmodium berghei*. In this article, we report that a secretory microneme protein, named cell-traversal protein of *Plasmodium* ookinetes and sporozoites (CelTOS), has a crucial role in the cell-traversal ability of both these stages. We show that CelTOS is necessary for both stages to break through cellular barriers and establish infection in the new host.

Results

Expressed sequence tags of the celtos gene are present in two different host-invasive stages

To search for genes involved in parasite invasive motility, EST databases of two motile stages, salivary gland sporozoites and ookinetes, of *P. berghei* were used (Yuda *et al*., 2001; Ishino *et al*., 2004). EST sequences of the respective stages were separately assembled into contigs and were screened for genes encoding micronemal proteins, using sequences representing the N-terminal signal peptide as probes. A contig encoding a 25 kDa protein with a secretory protein-like structure was found in both databases and named CelTOS. The numbers of *celtos* ESTs in the ookinete and sporozoite databases were five (of 11 814 ESTs) and 10 (of 3825 ESTs) respectively. This suggests that an identical molecule acts in the malarial invasion of the two hosts, a possibility that was not anticipated. Therefore, this gene was investigated further. Study of *Plasmodium* genome databases (PlasmoDB) indicated that orthologous genes are present in several plasmodium species, including the medically important parasites, *Plasmodium falciparum* and *Plasmodium vivax* (Fig. 1). On the other hand, a sequence similarity search of DNA databanks showed that CelTOS has no significant similarity to other known proteins. These results indicate that the *celtos* gene evolved in a common ancestor of *Plasmodium* parasites.

CelTOS is produced by the ookinete and the liver-infective sporozoite and is localized to micronemes

To investigate the expression profile of the CelTOS gene

```
P. berghei      1 MNKLTKLSVISSVF-VFFCFFNVLCLRGKNGSEMSSFLEGGVESS
P. vivax        1 MNKVNRVSIICA-FLALFCFVNVLSLRGKSGSTASSSLEGGSEFS
P. falciparum   1 MNALRRLPVICS-FLVFLVFSNVLCFRGNNGHNSSSSLYNGSQFI

P. berghei     45 NRIKKSLAS-FISESSSLDDIGNGLAETITNEIFSAFQQDSSSFL
P. vivax       45 ERIGNSLSS-FLSESASLEVIGNELADNIANEIVSSLQKDSASFL
P. falciparum  45 EQLNNSFTSAFLESQ-SMNKIGDDLAETISNELVSVLQKNSPTFL

P. berghei     89 QTKFDIKKHIKENAKKVLIEAIRLGLEPVEKIVAQSIQPPKVNRH
P. vivax       89 QSGFDVKTQLKATAKKVLVEALKAALEPTEKIVASTIKPPRVSED
P. falciparum  89 ESSFDIKSEVKKHAKSMLKELIKVGLPSFENLVAENVKPPKVDPA

P. berghei    134 TYSLVSPVVKALFNKIEEAVHKPVSDNIWDYAGGDDEYE-ETEED
P. vivax      134 AYFLLGPVVKTLFNKVEDVLHKPIPDTIWEYESKGS-LEEEEAED
P. falciparum 134 TYGIIVPVLTSLFNKVETAVGAKVSDEIWNYNSPDVSESEESLSD

P. berghei    178 NFDNDFFN
P. vivax      178 EFSDELLD
P. falciparum 179 DFFD----
```

Fig. 1. A comparison of amino acid sequences of *P. berghei* CelTOS, *P. falciparum* and *P. vivax* orthologues. The deduced amino acid sequence of *P. berghei* CelTOS was aligned with that of *P. falciparum* CelTOS (PlasmoDB identifier PFL0800c) and *P. vivax* CelTOS. Gaps are introduced to obtain optical matching by using GENETIX-MAC software. Conserved residues are boxed. The amino acid numbers from the first Met residue are shown on the left of each line. The predicted N-terminal signal sequence is underlined.

in the malarial life cycle, a polyclonal antibody was prepared against recombinant protein produced in *Escherichia coli*, and indirect immunofluorescent analysis was performed in different motile stages. Positive signals were observed in the ookinete and salivary gland sporozoite (Fig. 2A). However, CelTOS was not detected in the intraerythrocytic stages by either indirect immunofluorescent analysis (Fig. 2A) or Western blot analysis (data not shown). The detected signals were mainly observed in the apical cytoplasm, suggesting localization to micronemes. CelTOS was not detected in the oocyst sporozoite, the mosquito salivary gland-infective stage. This indicates that sporozoites start to produce this protein again after salivary gland infection.

The *in vitro* expression profile of *celtos* during ookinete development was investigated by Western blot analysis (Fig. 2B). CelTOS first appeared 10 h after fertilization and increased with ookinete development. In the early phase (10 h), a protein with the same molecular mass as the N-terminal signal peptide-processed form (20 kDa) was detected. It was then gradually replaced by a smaller protein (17 kDa). This finding suggests that processing of the N-terminal region occurred during maturation to the secreted form as reported for other microneme proteins of apicomplexan parasites (Soldati *et al*., 2001).

Immunoelectron microscopy of mature ookinetes revealed that CelTOS is localized to the micronemes (Fig. 2C). The gold particles were localized to the micronemes of relatively high electron density and were mainly distributed within them, not at the edges. Interestingly, this localization pattern is consistent with that of the von Willebrand factor-related adhesive protein, a putative secretory microneme protein with an adhesive protein-related motif (Yuda *et al*., 2001), and contrasts with that of CTRP, a paralogous protein of TRAP, which is mainly detected at the edge of the microneme probably due to integration into the microneme membrane (Yuda *et al*., 2001). The distinct distribution patterns of CelTOS and CTRP suggest that CelTOS is secreted directly into the cytoplasm of the midgut epithelial cell, while CTRP may be first presented on the ookinete surface and then released, as TRAP is thought to be in the sporozoite stage (Kappe *et al*., 1999).

Western blot analysis of the sporozoite stage confirmed that CelTOS is produced by the sporozoite in the salivary gland, but not by the sporozoite in the oocyst (Fig. 2D). Immunoelectron microscopy indicated that CelTOS is localized to micronemes of the salivary gland sporozoite (Fig. 2E). The size of the protein detected by Western blot analysis was smaller than that of the recombinant protein (N-terminal signal peptide-processed form) and was the same as that detected in the mature ookinete (17 kDa, Fig. 2B). As mentioned above, this suggests that the N-terminal portion of this protein underwent further processing. The specific production in the liver-infective sporozoite

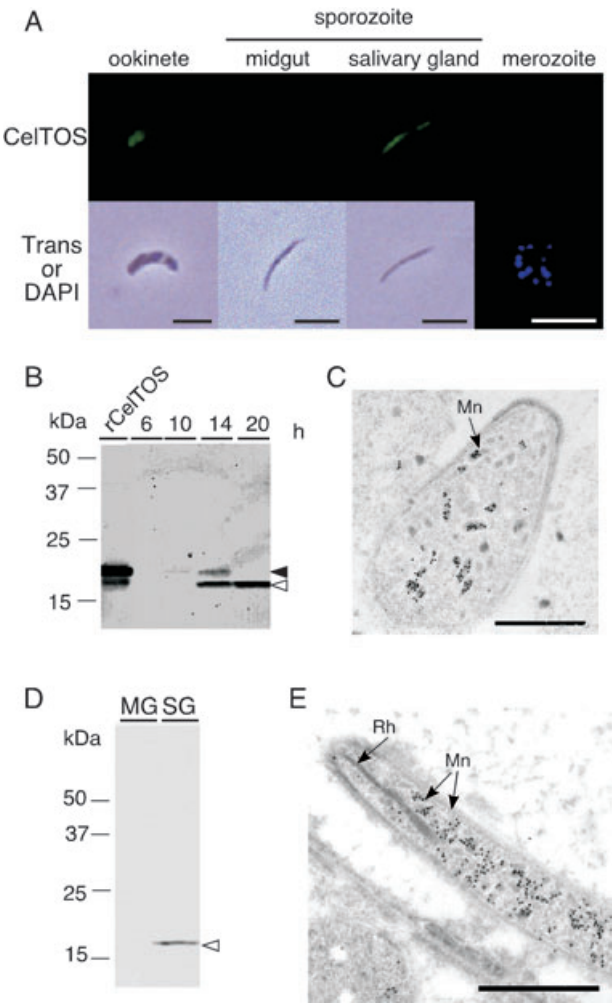

Fig. 2. CelTOS is produced by both mosquito midgut- and mammalian liver-infective stages and localized to the micronemes.
A. Expression profile of the CelTOS gene in host-invasive stages of the malarial parasite. Immunofluorescent microscopy was performed in different host invasive stages, including ookinetes, midgut sporozoites, salivary gland sporozoites and merozoites. Signals were detected using anti-CelTOS antibodies and secondary antibodies conjugated with FITC. Transilluminated (Trans) or 4′,6-diamidino-2-phenylindole staining (DAPI) images are shown in lower panels.
B. CelTOS production during ookinete development. Infected blood was cultured at 20°C in ookinete culture medium. After the time (h) indicated over each lane, the same volume was collected from the culture, and CelTOS production was studied by Western blot analysis using the same primary antibodies as in A. rCelTOS, recombinant signal peptide-processed form, which was produced by *E. coli*.
C. CelTOS is localized in the ookinete to micronemes. Localization of CelTOS was examined by immunoelectron microscopy with the same primary antibodies as in A and the secondary antibodies conjugated with gold particles (10 nm in diameter). The particles were localized to micronemes of high electron density.
D. CelTOS is produced by the sporozoite after salivary gland infection. Midgut sporozoites and salivary gland sporozoites were collected 24 days after an infective blood meal. The production of CelTOS was investigated in both stages (3×10^5 parasites each) by Western blot analysis.
E. CelTOS is localized to micronemes of the salivary gland sporozoite. Mosquito salivary glands were dissected 24 days after an infective blood meal and immunoelectron microscopy was performed as in C. Bars represent 5 μm.

and the localization to micronemes strongly suggest that CelTOS has a role in malarial transmission to the vertebrate host.

CelTOS is secreted during sporozoite movement and left behind as a trail

Malarial sporozoites exhibit a circular movement on a glass slide. This is called gliding motility, because it proceeds without changing the cell shape. While gliding on a slide, they secrete micronemal contents from the apical pole and leave them behind as a trail (Sultan *et al.*, 1997; Stewart and Vanderberg, 1988). Because this trail contains TRAP, a major microneme protein of the sporozoite, it can be visualized on the glass slide by immunofluorescent staining with anti-TRAP antibodies (Fig. 3, lower right). To examine the secretion of CelTOS during sporozoite movement, immunofluorescent microscopy was performed with anti-CelTOS antibodies (lower left). Trails were visualized on the slide with a periodic, discontinuous appearance, indicating its secretion from individual micronemes. Notably, the trails were broader and not as sharp as those stained with anti-TRAP antibodies. When the parasite plasma membrane was not permeabilized after fixation with paraformaldehyde, CelTOS was not detected at the apical tip or on the parasite surface (upper left). In contrast, TRAP was capped at the apical tip in some of the sporozoites (upper right). These results indicate that CelTOS is deposited on a glass slide directly as an insoluble material, while TRAP might be first presented on the parasite surface and then released from the posterior end, leading to the formation of relatively sharp trails. This assumption correlates well with secretory protein-like (CelTOS) and membrane protein-like (TRAP) molecular structures of the respective proteins. As discussed later, the distinct secretion patterns between CelTOS and TRAP might reflect their functions in the parasite cell-passage machinery.

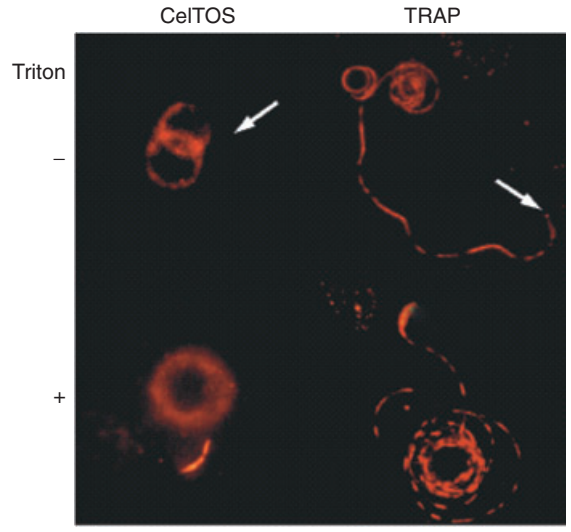

Fig. 3. CelTOS is deposited as a trail during sporozoite gliding. Salivary gland sporozoites were allowed to glide in chamber slides at 37°C for 1 h and fixed with paraformaldehyde, followed (Triton +) or not followed (Triton –) by permeabilization. The slides were stained with the primary antibodies, anti-CelTOS (CelTOS) or anti-TRAP (TRAP), and secondary antibodies labelled with Cy3. Trails detected by anti-TRAP antibodies had a sharper appearance than those detected by anti-CelTOS antibodies. Parasites were not stained by anti-CelTOS antibodies when not permeabilized, while some of them were stained by anti-TRAP antibodies. Arrows indicate the apical tip of the sporozoite.

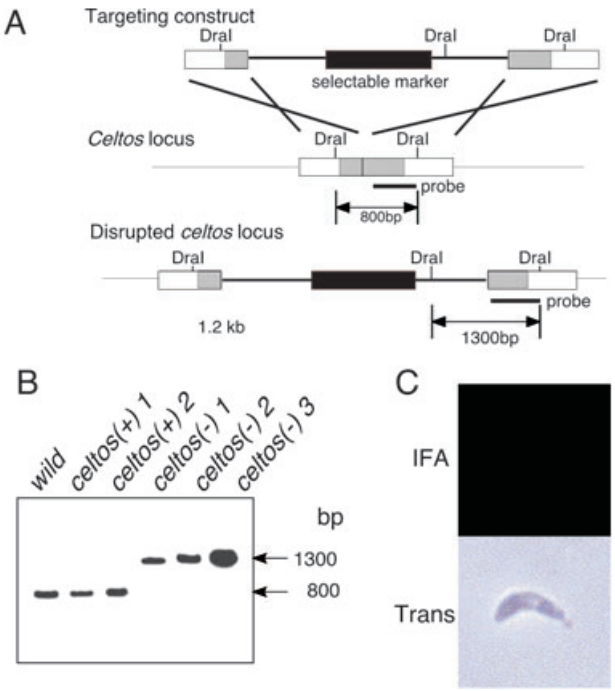

Fig. 4. Targeted disruption of the CelTOS gene.
A. Schematic representation of targeting procedure. The targeting vector (top) containing a selectable marker gene is integrated into the CelTOS gene locus (middle) by double crossover recombination. This recombination event resulted in the disruption of the *celtos* gene and conferred pyrimethamine resistance to the disruptants (bottom).
B. Genomic Southern hybridization of wild-type (WT) and *celtos*(–) populations. Genomic DNA isolated from the respective parasite populations was digested with DraI and hybridized with the probe indicated in (A) by a solid bar. Integration of the targeting construct increased the size of the detected fragments from 0.8 to 1.3 kb.
C. Immunofluorescent analysis of the *celtos*-disrupted ookinete. *celtos*-disrupted ookinetes were collected from the culture and stained with primary antibodies against CelTOS followed by FITC-conjugated secondary antibodies. Compare with Fig. 1A.

Construction of CelTOS gene-disrupted parasite clones

To investigate the function of CelTOS in the malarial life cycle, *celtos*-disrupted parasites were prepared. Figure 4A shows the knock-out vector used. It is

composed of a selectable marker gene that confers resistance to the antimalarial drug, pyrimethamine and DNA fragments of the gene ligated to both ends. This construct was introduced into merozoites by electroporation, and merozoites with this construct integrated into the genome were selected using pyrimethamine. Clones were isolated by limiting dilution. Disruption of the target gene of each clone was confirmed by Southern blot (Fig. 4B) and polymerase chain reaction (PCR) analyses (data not shown). Clones were obtained from two individual experiments to confirm that the disruptants used for the following experiments were not the same clone.

In the intra-erythrocytic stages, the *celtos*-disrupted parasites had no phenotypic differences from wild-type parasites. Growth rates in rat blood were similar for disruptants and wild types (data not shown). This indicates that CelTOS is not essential for the parasite's proliferation in the vertebrate host blood, consistent with the observation that this protein is not produced by intra-erythrocytic stages.

CelTOS has a critical role in ookinete infection of the mosquito midgut

Ookinetes are generated in the midgut lumen and traverse epithelial cells from the luminal to the basal side. They then attach to the basal lamina of the epithelial cell and transform to oocysts. Malarial sporozoites are released from the oocysts into the mosquito's haemolymph 2–3 weeks after an infective blood meal. The sporozoites invade the salivary gland, pass through the gland cells and gather in the lumen, where they acquire the ability to infect the mammalian liver.

celtos-disrupted parasites showed normal exflagellation rates and normally developed into ookinetes *in vivo* and *in vitro* (data not shown). To assess the effect of gene disruption on parasite development in the mosquito, oocyst formation and sporozoite numbers in the midgut, haemolymph and salivary glands were examined (Table 1). *celtos*-disruption decreased the number of oocysts formed on the midgut by approximately 200-fold. Correspondingly, sporozoites in the midgut were decreased to approximately 1/100 of wild-type parasites. Sporozoites in the salivary gland were also decreased. This reduction can be attributed solely to the reduced sporozoite number in the midgut, because the ratio of salivary gland sporozoites to midgut sporozoites was higher in disruptants (0.49–0.93) than in wild-type parasites (0.15–0.20). These results indicate that CelTOS has a critical role in ookinete infection of the mosquito midgut, but does not participate in sporozoite infection of the salivary gland, consistent with the observation that CelTOS is produced by ookinetes, but not by sporozoites before salivary gland infection.

CelTOS has a critical role in sporozoite infection of the liver

In the mosquito salivary gland, sporozoites acquire the ability to infect a mammalian host. CelTOS is also produced in this stage. In light and electron microscopic observations of the salivary gland sporozoite, there were no obvious morphologic differences between the wild-type parasite and the disruptant. Furthermore, the ratio of motile to non-motile sporozoites was similar to that of the wild-type parasite, indicating that the secretion of micronemes was not affected by *celtos*-disruption. To assess the influence of the disruption on sporozoite infectivity to the liver, the salivary gland sporozoites were injected intravenously into rats, and the infection rate and the period necessary for apparent parasitaemia (prepatent days) were compared between disruptant and wild-type parasites (Table 2). After injection of 1000 wild-type sporozoites, all rats were infected, but when rats were injected with the disruptant, some rats were not infected. Furthermore, prepatent days for apparent parasitaemia of the infected rats were significantly longer with the disruptant than the wild type. By comparing prepatent days and infection rates determined by injection of various numbers

Table 1. Development of *celtos*-disrupted parasites in *Anopheles stephensi* mosquitoes.

Parasite population	No. of oocysts/ mosquito	No. of sporozoites/mosquito		
		Midgut	Haemolymph	Salivary gland
Wild-type	278 ± 43	63 101 ± 3845	4036 ± 562	11 222 ± 1900
celtos (+) 1	408 ± 99	93 560 ± 12 900	4694 ± 624	13 783 ± 2098
celtos (+) 2	249 ± 61	77 950 ± 4600	4747 ± 366	15 547 ± 2904
celtos (–) 1	1 ± 0.2	1 058 ± 220	98 ± 31	520 ± 126
celtos (–) 2	2 ± 0.1	761 ± 100	78 ± 7	383 ± 69
celtos (–) 3	1 ± 0.4	538 ± 160	134 ± 60	503 ± 195

Anopheles stephensi mosquitoes were fed on infected mice. On day 14 post feeding, oocysts formed in the midgut were counted under the microscope. On day 20, sporozoites in the midgut, haemolymph and salivary glands were separately collected and counted. Each value is the mean from at least three independent experiments with its standard error.

Table 2. Infectivity of wild-type and disruptant sporozoites to rats.

Parasite population	No. of injected salivary gland	Sporozoites infection rate[a]	Prepatent period of infection[b] (days)
Wild-type	1000	5/5	3.0
	100	5/5	4.2
	50	5/5	4.6
	20	5/5	4.6
	10	4/5	5.0
celtos (+) 1	1000	5/5	3.4
celtos (+) 2	1000	5/5	3.4
celtos (–) 1	1000	8/10	4.8
celtos (–) 2	1000	9/10	4.7
celtos (–) 3	1000	10/10	4.7

a. Number of infected rats/number of rats inoculated with salivary gland sporozoites.
b. Number of days between sporozoite inoculation and detection of at least one erythrocytic stage upon a 10 min examination of a Giemsa-stained blood smear.
Sporozoite infectivity in rats was assessed by infection rates and prepatent periods. Three-week-old Wistar rats were intravenously injected with 0.2 ml of sporozoite suspensions in Medium 199. Parasitaemia was checked daily by Giemsa-stained blood smears.

of wild-type sporozoites (Table 2), the infectivity of the disruptant was estimated to be ~1/20 to ~1/50 of the wild type.

celtos*-knockout sporozoites are impaired in cell-passage ability*

Sporozoites show two types of cell invasion *in vitro*, 'infection' and 'passage' (Mota *et al*., 2001). Because microneme proteins have a central role in parasite motility, cell-invasion motility of disruptant sporozoites was examined using *in vitro* assays. Hepatocyte-infection ability of the disruptants was assessed in a human hepatoma-derived cell line, HepG2 (Hollingdale *et al*., 1981). Sporozoites were added to a culture of HepG2 cells and the number of exoerythrocytic forms (EEFs) produced was compared between wild-type parasites and disruptants. The numbers of EEFs were similar for both (Fig. 5A), indicating that CelTOS is not necessary for sporozoite infection of the hepatocyte.

Cell-passage activity was then measured using a cell wound assay (Mota *et al*., 2001). Sporozoites were added to HeLa cells, and cells wounded by sporozoite penetration were identified by uptake of fluorescein isothiocyanate (FITC)-conjugated dextran from the medium. The number of wounded cells was greatly decreased in HeLa cells treated with disruptants (Fig. 5B), almost to the level of HeLa cells treated with heat-inactivated negative controls, indicating that this ability is severely damaged by the gene disruption. Taken together, these results demonstrated that CelTOS is a microneme protein specifically involved in parasite cell passage.

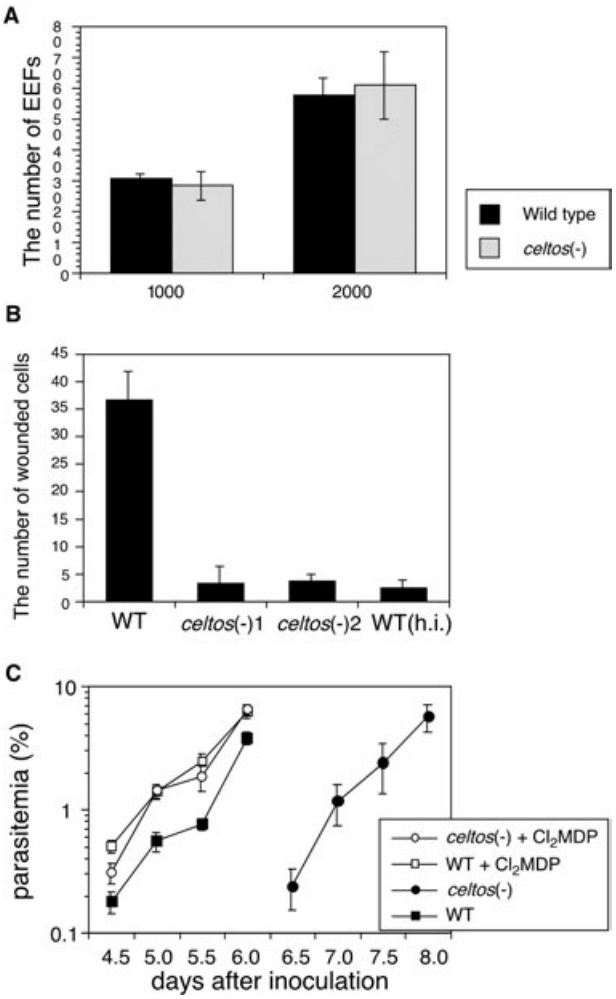

Fig. 5. c*eltos*-disrupted sporozoites are impaired in cell-passage activity.
A. *celtos*-disruption does not affect sporozoite ability to infect hepatocytes. Salivary gland sporozoites (1000 or 2000 per well) were added to HepG2 cells and cultured for 48 h. Formed EEFs were counted after immunofluorescence staining with antiserum against CS protein. EEF numbers were compared between disruptants [*celtos*(–) 1] and wild-type (WT) parasites. Data are mean numbers of EEFs per well with standard errors from at least five independent experiments.
B. *celtos*-disrupted sporozoites are impaired in cell-passage activity. Salivary gland sporozoites (3000 per well) were added to HeLa cells and incubated for 1 h with FITC-conjugated dextran (1 mg ml^{-1}). Cell-passage activity was estimated by the number of cells wounded by sporozoite passage, which were identified by cytosolic labelling with FITC-conjugated dextran. Numbers of positive cells were compared between disruptants [*celtos*(–) 1] and wild-type (WT) parasites. Data are mean numbers of FITC-positive cells in one-fifth area of a well with standard errors from at least three independent experiments.
C. Restoration of *celtos*(–) sporozoite infectivity to the liver in Kupffer cell-depleted rats. Liposome-encapsulated Cl_2MDP (filled) or PBS (open) was injected intravenously into rats. After 48 h, 3000 sporozoites of *celtos*(–) 1 (circles), *celtos*(–) 2 (triangles), or wild-type (squares) populations were inoculated intravenously. Parasitaemia in each rat was checked by Giemsa-stained blood smears after inoculation on the days indicated. Kupffer cell depletion in rats resulted in almost equal sporozoite infectivity between disruptants and wild types. Values shown represent the mean parasitaemia (± SEM) of five rats.

Depletion of Kupffer cells restored disruptant's infectivity to the rat liver

We recently demonstrated that sporozoite cell-traversal motility is necessary to cross the liver sinusoidal cell layer (Ishino *et al*., 2004). The results of the *in vitro* assays therefore suggest that the liver infectivity of the disruptants was decreased at this step. To test this possibility, we studied the liver infectivity of disruptants in Kupffer cell-depleted rats (Vreden *et al*., 1993; Van Rooijen and Sanders, 1994), in which sporozoites can pass freely through the sinusoidal cell layer without cell passage (Ishino *et al*., 2004). The *celtos*-disrupted sporozoites were intravenously inoculated into normal rats, and parasitaemias during the exponential growth period (from 3.5 to 5.0 days after inoculation) were compared with that of the wild type (Fig. 5C). The increase of parasitaemia occurred approximately 1.5 days later with the disruptants than with the wild type. This result agrees with the data on prepatent days (1.3–1.4 days later in disruptants, Table 2). In contrast, when inoculated into Kupffer cell-depleted rats, parasitaemias were almost equal for both strains. These results demonstrate that CelTOS is necessary for cell passage required to cross the sinusoidal layer.

CelTOS is involved in ookinete passage through mosquito midgut epithelial cells

The sporozoite results suggest that *celtos*-disruption impaired ookinete cell traversal and led to a reduction in midgut infectivity. To investigate the step in which midgut infection was affected by *celtos*-disruption, mosquitoes were dissected 21 h after an infective blood meal, when most wild-type ookinetes were expected to have finished migrating to the basal lamina, and the location of ookinetes in the midgut epithelium was examined by transmission electron microscopy (Table 3 and Fig. 6).

When mosquitoes were infected with wild-type parasites, 50 ookinetes were found in the midgut epithelium (in 254 ultrathin sections from four midguts). Among them, 28 ookinetes had already finished passage through the epithelium and attached to the basal lamina at their apical end (Fig. 6A). Furthermore, 21 ookinetes were inside epithelial cells, nine of them potentially attached to the basal lamina because they were located near the basal lamina with the apical end directed to the basal side. One ookinete was found on the luminal side of an epithelial cell with its anterior half projecting into the cell.

When mosquitoes were infected with disruptants, 52 ookinetes were found in the midgut epithelium (in 302 sections from four midguts). There were no ookinetes clearly attached to the basal lamina. Only six ookinetes were potentially attached to the basal lamina, and another 39 in epithelial cells apparently failed to complete their migration, because they were in damaged cells nearly (or completely) detached from the epithelial cell wall (Fig. 6B) or remained intracellular far from the basal lamina (Fig. 6C). Seven ookinetes were on the luminal surface of the epithelial cell and four of them had their apical tip projecting into the epithelial cell (Fig. 6D). These results demonstrated that CelTOS is necessary for the ookinete to migrate through the cytoplasm of the midgut epithelial cell to the basal lamina.

Table 3. Distribution of wild-type and disruptant ookinetes in the mosquito midgut epithelium.

	Wild-type	Disruptant
Cell surface[a]	0	3
Apical membrane[b]	1	4
Cytoplasm[c]	21 (9)[d]	45 (6)[d]
Basement membrane[e]	28	0
Total	50	52

a. Number of ookinetes in the microvilli, but did not invade the epithelium.
b. Number of ookinetes penetrating the apical cell membrane.
c. Number of ookinetes in the cytoplasm.
d. Number of ookinetes observed in the cytoplasm, but whose arrival at the basal lamina could not be determined.
e. Number of ookinetes attached to the basal lamina.
Mosquitoes were fed on infected mice and dissected 21 h after blood meal. Ookinete location in the mosquito midgut epithelium was analysed by transmission electron microscopy and compared between wild types and disruptants.

Discussion

Mosquito midgut and vertebrate liver invasion are obligatory steps for the malarial parasite to establish infection in new hosts. In this article, we demonstrated that a microneme protein, CelTOS, is produced by parasites at these distinct host-invasive stages and has a critical role in breaking through the cellular barriers against them. In both stages, CelTOS is involved in cell-traversal ability of the parasite, suggesting that conserved mechanisms for cell traversal are used by both stages.

In the ookinete stage, *celtos*-disrupted ookinetes stopped during passage to the basal lamina and remained in the cytoplasm of the damaged epithelial cells. This phenotype indicates that CelTOS is involved in the step after ookinetes rupture the cell membrane, i.e. migration through the cytoplasm. The number of ookinetes that invaded the midgut epithelial cells was similar for *celtos*-disruptants and wild type, suggesting that *celtos*-disrupted ookinetes could migrate to the cytoplasm of epithelial cells as well as wild type. Similarly, *celtos*-disrupted sporozoites are severely impaired in cell-traversal ability, although they showed normal gliding motility *in vitro* and infected hepatocytes in the same efficiency as wild type. These results indicate that gliding motility of the disruptants is

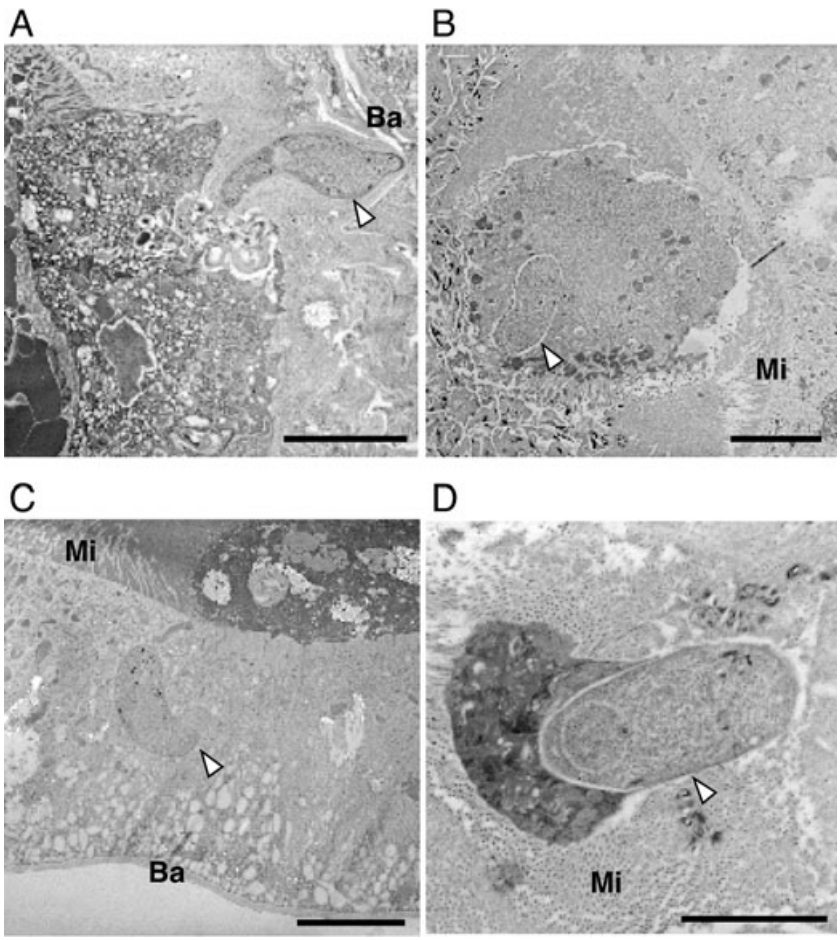

Fig. 6. *celtos*-disrupted ookinetes fail to migrate through the midgut epithelium.
A. a wild-type ookinete that travelled through the epithelium and attached to the basal lamina at the apical end. This ookinete might have first invaded the epithelial cell at the left side, which is severely damaged and strongly stained, and then migrated to the adjacent cell that the ookinete is seen penetrating. The attachment of the parasite apex to the basement membrane (Ba) is clearly demonstrated in this section.
B. *celtos*-disrupted ookinete (arrowhead) has been ejected from the epithelium with the damaged cell it invaded. The cell begins to collapse. Mi, microvilli.
C. *celtos*-disrupted ookinete (arrowhead) resides in an epithelial cell. The invaded cell lost microvilli but appears relatively intact. This ookinete might have entered the epithelium from the cell at the upper right, which is strongly stained and protrudes from the epithelium, and then migrated to this cell laterally.
D. *celtos*-disrupted ookinete (arrowhead) inserts its apical end into the epithelial cell. The invaded cell is strongly stained and protrudes over the microvilli (Mi) of neighbouring intact cells, indicating that it ruptured the epithelial cell membrane, but failed to move forward into the cytoplasm. Bars represent 5 μm.

not impaired in both stages. Thus, CelTOS may be a micronemal protein solely required for cell traversal.

We have previously proposed that that SPECT and SPECT2 are essential for sporozoite cell-passage activity (Ishino *et al*., 2004; 2005). *spect*- and *spect2*-disruptants completely lack cell-wounding activity, suggesting that these two proteins are essential for a step preceding sporozoite invasion into the cytoplasm, such as attachment to the host cell surface or rupture of the plasma membrane. Contrary to these disruptants, *celtos*-disruptants seem to retain weak cell-wounding activity in the sporozoite stage, which was suggested by the result that the average number of wounded cells was slightly higher with *celtos*-disruptants than with heat-inactivated wild-type sporozoites (Fig. 5B). In the present study, however, this observation could not be confirmed due to the very small number of disruptant sporozoites obtained from infected mosquitoes (approximately 1/100 of the wild type). To address this problem, we recently prepared a recombinant parasite with the upstream region of the CelTOS gene substituted with that of the WARP (von Willebrant factor A domain-related protein) gene, which is specifically expressed in the ookinete stage (Yuda *et al*., 2001). This mutant parasite expressed *celtos* in the ookinete stage and produced enough sporozoites for further studies. The preliminary results obtained with this parasite confirmed that a small proportion of the disruptant sporozoites can traverse culture cells. This suggests that CelTOS acts at a different step than SPECTs in cell traversal. It is possible that *celtos*-disrupted sporozoites proceed to the cytoplasm of invaded cells but remain intracellular as *celtos*-disrupted ookinetes, resulting in severe reduction of cell-passage activity.

TRAP-family proteins are microneme proteins produced in both ookinete and sporozoite stages and are essential for parasite gliding motility. They are translocated to the parasite surface and move on the surface from the anterior to the posterior side, generating forward movement of parasites. If gliding motility of *celtos*-disrupted parasites is normal, it would implies that surface movement of microneme proteins is not impaired. The impaired cell-passage ability therefore could be due to a failure of anchoring this surface movement to the cytoplasm of the host cell. We speculate that CelTOS is a candidate protein that may play this role by interacting with molecules in the cytoplasm. It is possible that the different trail patterns

between TRAP and CelTOS might represent the different functions between these molecules in the parasite mobility machinery.

In summary, CelTOS is the first microneme protein that was shown to be critical for cell traversal in both ookinetes and sporozoites. Its fate after secretion from micronemes and the phenotype of the disruptants suggest that its role in cell traversal is unique among micronemal proteins. Further investigation of this protein therefore may provide new insight into the molecular mechanisms of cell traversal by malarial parasites.

Experimental procedures

Parasite preparations

BALB/c mice infected with *P. berghei* ANKA strain were prepared by peritoneal injection of infected blood stored at −70°C. For ookinete culture, blood was collected by cardiac puncture from infected mice within one blood passage. Culturing was performed as described previously (Yuda *et al*., 1999b). Cultured ookinetes were purified by erythrocyte lysis in 0.83% NH_4CL and used for further analysis. For construction of a cDNA library, cultured ookinetes were purified by density gradient centrifugation using Nicoprep 1.077 A (AXIS-SHIELD PoC AS, Oslo, Norway).

For mosquito biting, infected mice were used within one blood passage. At 20–24 days after the infective blood meal, mosquitoes were anaesthetized in CO_2 and sporozoites in the haemolymph, midgut and salivary glands were collected separately, as described previously (Kariu *et al*., 2002). Briefly, the haemolymph was collected from a pinhole in the abdomen by injection of 10 μl of Medium 199 (Invitrogen, Carlsbad, CA, USA), into the body cavity. Then the salivary glands and the midgut were dissected out, washed in saline, and collected separately in 70 μl of Medium 199 on ice. The collected tissues were gently ground in the medium to release sporozoites and centrifuged at 18 *g* for 3 min to remove tissue fragments. Sporozoites in the supernatant were counted using a haemocytometer and used for further analysis.

Nucleic acid sequences of human Plasmodium *parasites*

Sequence data for *P. falciparum* chromosome 12 were obtained from the Stanford DNA Sequencing and Technology Center website at http://www-sequence.stanford.edu/group/malaria. Sequence data for *P. vivax* were obtained from http://plasmodb.org/restricted/data/P_vivax/YAC/.

Antibody preparation and Western blot analysis

A DNA fragment encoding the signal peptide-processed form of CelTOS (amino acid residues 24–185) was amplified by PCR by the primer pair, 5′-CGGGATCCTTGAGAGGCA AAAATGGATCAGAA-3′ and 5′-CGGCTCGAGTCAATTAAA GAAATCATTATCGAAG-3′, using *P. berghei* genomic DNA as a template. This fragment was digested with BamHI and XhoI and then subcloned into the *E. coli* expression vector pGEX 6P-1 (Amersham Pharmacia Biotech, Piscataway, NJ). Recombinant protein was produced in an *E. coli* strain, BL21, as a glutathione S-transferase (GST) fusion protein, purified with a glutathione column, and used for immunization of rabbits. Antibodies against GST were removed from the antisera by incubation with GST-conjugated Sepharose. Specific antibodies were affinity-purified using an NHS-activated High Trap column (Amersham Pharmacia Biotech) linked with the GST-fused recombinant protein. For preparation of anti-*P. berghei* circumsporozoite (CS) protein antisera, a synthetic peptide, DPPPPNANDPAPPNANC (amino acid residues 132–147), was conjugated to keyhole limpet haemocyanin and used for immunization of rats.

For Western blot analysis, purified parasites were homogenized in SDS-PAGE sample buffer containing 1% SDS and 5% 2-mercaptoethanol and were boiled for 5 min. Recombinant CelTOS was separated from fused GST by treatment with processing protease, PreScission Protease (Amersham Pharmacia Biotech) and was boiled in the same buffer. These samples were separated by SDS-PAGE on a 10–20% gradient gel and electrophoretically transferred to a nitrocellulose membrane. The blotted membrane was blocked in phosphate-buffered saline (PBS) containing 5% skimmed milk, incubated for 60 min with purified anti-CelTOS antibodies diluted in the same buffer (20 μg ml^{-1} final concentration), washed and then incubated for 60 min with alkaline phosphatase-conjugated anti-rabbit IgG (Bio-Rad, Hercules, CA) diluted 1:1000 in the same buffer. After washing, signals were obtained using the AP Conjugate Substrate Kit (Bio-Rad).

Immunofluorescence microscopy

Immunofluorescence microscopy was performed as described previously (Yuda *et al*., 1999b). Briefly, purified parasites on glass slides were fixed in acetone for 2 min and rinsed in PBS. The slides were then blocked in PBS containing 1% bovine serum albumin (BSA), incubated for 60 min with purified anti-CelTOS antibodies diluted in the same buffer (20 μg ml^{-1} final concentration). After being rinsed five times in PBS, the slides were incubated for 60 min with FITC-conjugated anti-rabbit IgGs (Zymed, South San Francisco, CA) diluted 1:40 in the same buffer, and again rinsed five times in PBS. For nuclear staining, 4′,6-diamidino-2-phenylindole staining (DAPI, 0.02 μg ml^{-1} final concentration) was added to the secondary antibody solution. Immunofluorescence analysis of sporozoite gliding trails was performed as follows. Sporozoites were suspended in Medium199 containing 3% BSA, spotted on multi-well slides, and incubated for 1 h at 37°C. Before staining, slides were washed in PBS, fixed in 4% paraformaldehyde for 5 min, and rinsed in PBS. Samples were mounted in PermaFluor (Immunotech, Marseille, France), and micrographs were obtained with an Olympus BX60 fluorescence microscope (Plympus, Tokyo, Japan) with a C4742-95 digital colour camera (Hamamatsu Photonic System, Hamamatsu, Japan). The images were processed using AquaCosmos (Hamamatsu Photonic System) and Adobe Photoshop (San Jose, CA).

Immunoelectron microscopy

For transmission electron microscopy analysis, mosquito

midguts were dissected at 21 h after an infected blood meal, fixed in 0.1 M phosphate buffer (pH 7.4) containing 1% paraformaldehyde-2.5% glutaraldehyde (TAAB, Berkshire, UK) for 90 min on ice. They were dehydrated in ethanol and embedded in LR White resin (London Resin Company, London, UK). A sequence of ultrathin sections was obtained from the posterior portion of the midgut (~70 sections per midgut) and stained with 2% uranyl acetate and Reynold's lead citrate. Ookinetes around the epithelium were examined in each section under a transmission electron microscope.

Immunoelectron microscopy was performed as described previously (Yuda *et al*., 2001). Briefly, purified parasites were fixed in 0.1 M phosphate buffer (pH 7.4) containing 1% paraformaldehyde-0.1% glutaraldehyde (TAAB) for 15 min on ice. They were dehydrated in ethanol and embedded in LR Gold resin. Ultrathin sections were blocked for 30 min in PBS containing 0.01% Tween 20 and 5% non-fat dry milk (blocking buffer), incubated at 4°C overnight with primary antibodies (20 μg ml^{-1} final concentration), and then incubated for 1 h with goat anti-rabbit IgG conjugated to gold particles (15 nm diameter; AuroProbe: Amersham Pharmacia Biotech) diluted 1:40 in blocking buffer, and washed six times. Finally, the sections were fixed with 2.5% glutaraldehyde for 10 min and stained with 2% uranyl acetate and Reynold's lead citrate.

Targeted disruption of the P. berghei *gene*

The targeting vector for the gene was constructed as follows. Two partial DNA fragments of the gene were amplified by PCR using genomic DNA as template with the primer pairs: 5′-GGCGAGCTCTATCTTTAATTTTTATTTTGTA-3′ and 5′-GCCGGATCCACATAGAACATTAAAAAAGCAAAA-3′, 5′-GGCCTCGAGTTGAGAGGCAAAAATGGATCAGAA-3′ and 5′-GCCGGTACCTTACGATTATCACTTAATGTTGTT-3′. These fragments were subcloned into either side of the selectable marker gene in pBluescript (Stratagene, La Jolla, CA) using the unique restriction sites, SacI/BamHI and XhoI/KpnI respectively. For the gene-targeting experiment, the plasmid was completely digested with the restriction enzymes, SacI and KpnI, to release the linear targeting construct. The gene-targeting experiment was performed as previously described (Yuda *et al*., 1999a).

Southern blot analysis

Southern blot analysis was performed essentially as described previously (Yuda *et al*., 1999a). Briefly, *P. berghei* genomic DNA extracted from blood stage parasites (2 μg) was completely digested with the restriction enzyme, DraI. The fragments were separated on 1.2% agarose gel and transferred to nylon membranes. Partial DNA fragments of the gene were amplified by PCR using genomic DNA as the template with the primer pair, 5′-CGGGATCCTTGAGAG GCAAAAATGGATCAGAA-3′ and 5′-CGGCTCGAGTCAAT TAAAGAAATCATTATCGAAG-3′. The products were labelled with [^{32}P]-dCTP and used as hybridization probes.

Assays of sporozoite gliding motility and infectivity in vitro

Gliding motility and infectivity of sporozoites were assessed using sporozoites collected from salivary glands 24 days after an infective blood meal. For the gliding motility assay, sporozoites were kept 2 h at 4°C in Medium 199 containing 3% BSA and then gliding on an uncoated microscope slide was observed under a phase-contrast microscope.

For the infectivity assay, sporozoites were intravenously injected into 3-week-old Wistar rats. The parasitaemia was checked daily by a Giemsa-stained blood smear, and infection rates and the prepatent period of infection were determined.

Sporozoite infection assay was performed out essentially as described (Cerami *et al*., 1992). Briefly, HepG2 cells were seeded in minimum essential medium with 10% fetal bovine serum, non-essential amino acids, 100 U ml^{-1} penicillin, and 100 g ml^{-1} streptomycin in 16-well chamber slides (Nunc, Napierville, IL) and cultured until they approached nearly confluence. Salivary gland sporozoites (1.0×10^3 or 2.0×10^3) were suspended in 100 μl of the same medium and added to each well. After incubation for 2 h, the medium was replaced with the same medium containing 3 mg ml^{-1} glucose. The cells were cultured another 48 h with changes of medium at 12-h intervals and were fixed in acetone for 2 min. EEFs formed were counted after immunofluorescent staining as described above using anti-CS protein antiserum and secondary antibodies conjugated with Cy3 (KPL, Gaithersburg, MD). At least three wells were counted in each experiment, and the results were expressed as mean values from five independent experiments.

Cell traversing activity assay

Cell-traversing activity of sporozoites was performed essentially as described previously (Ishino *et al*., 2004). Sporozoites (3.0×10^3) were added to HeLa cells seeded on an 8-well chamber slide and cultured for 1 h in the presence of 1 mg ml^{-1} FITC-labelled dextran (10 000 MW, lysine-fixable; Molecular Probes, Eugene, OR). The cells were incubated in complete culture medium for more than 1 h and fixed with 4% paraformaldehyde in PBS. FITC-positive cells were counted under a fluorescence microscope. Results were expressed as mean values from three independent experiments.

Depletion of rat Kupffer cells

Depletion of Kupffer cells was performed as previously described (Van Rooijen and Sanders, 1994). Briefly, 3-week-old female Wistar rats were injected intravenously with 120 μl of liposome-encapsulated clodronate or an equal volume of PBS as control. After 48 h, sporozoites (3.0×10^3) were injected into a tail vein and parasitaemia was checked by Giemsa-stained blood smear every 12 h. Elimination of Kupffer cells was confirmed by immunoperoxidase staining after liver perfusion with PBS, followed by fixation with 4% paraformaldehyde in PBS. Clodronate was a gift of Roche Diagnostics, Manheim, Germany.

Acknowledgements

We thank Gerard R. Wyatt for reading the manuscript. This

study was supported by a grant-in-aid for Scientific Research on Priority Areas to Y.C. (16017243,14207011,16659110) and to M.Y. (16390124, 16659111), of the Ministry of Education, Science, Culture, and Sports of Japan. It was also supported by grants from the Japan Science and Technology Agency to Y.C.

References

Blandin, S., Shiao, S.H., Moita, L.F., Janse, C.J., Waters, A.P., Kafatos, F.C., and Levashina, E.A. (2004) Complement-like protein TEP1 is a determinant of vectorial capacity in the malaria vector *Anopheles gambiae*. *Cell* **116:** 661–670.

Buscaglia, C.A., Coppens, I., Hol, W.G., and Nussenzweig, V. (2003) Sites of interaction between aldolase and thrombospondin-related anonymous protein in plasmodium. *Mol Biol Cell* **14:** 4947–4957.

Cerami, C., Frevert, U., Sinnis, P., Takacs, B., Clavijo, P., Santos, M.J., and Nussenzweig, V. (1992) The basolateral domain of the hepatocyte plasma membrane bears receptors for the circumsporozoite protein of *Plasmodium falciparum* sporozoites. *Cell* **70:** 1021–1033.

Dessens, J.T., Margos, G., Rodriguez, M.C., and Sinden, R.E. (2000) Identification of differentially regulated genes of *Plasmodium* by suppression subtractive hybridization. *Parasitol Today* **16:** 354–356.

Dobrowolski, J.M., and Sibley, L.D. (1996) Toxoplasma invasion of mammalian cells is powered by the actin cytoskeleton of the parasite. *Cell* **84:** 933–939.

Han, Y.S., and Barillas-Mury, C. (2002) Implications of Time Bomb model of ookinete invasion of midgut cells. *Insect Biochem Mol Biol* **32:** 1311–1316.

Hollingdale, M.R., Leef, J.L., McCullough, M., and Beaudoin, R.L. (1981) *In vitro* cultivation of the exoerythrocytic stage of *Plasmodium berghei* from sporozoites. *Science* **213:** 1021–1022.

Ishino, T., Yano, K., Chinzei, Y., and Yuda, M. (2004) Cell-passage activity is required for the malarial parasite to cross the liver sinusoidal cell layer. *Plos Biol* **2:** 77–84.

Ishino, T., Chinzei, Y., and Yuda, M. (2005) A *Plasmodium* sporozoite protein with a membrane attack complex domain is required for breaching the liver sinusoidal cell layer prior to hepatocyte infection. *Cell Microbiol* **7:** 199–208.

Jewett, T.J., and Sibley, L.D. (2003) Aldolase forms a bridge between cell surface adhesins and the actin cytoskeleton in apicomplexan parasites. *Mol Cell* **11:** 885–894.

Kaiser, K., Camargo, N., Coppens, I., Morrisey, J.M., Vaidya, A.B., and Kappe, S.H. (2004) A member of a conserved *Plasmodium* protein family with membrane-attack complex/perforin (MACPF)-like domains localizes to the micronemes of sporozoites. *Mol Biochem Parasitol* **133:** 15–26.

Kappe, S., Bruderer, T., Gantt, S., Fujioka, H., Nussenzweig, V., and Menard, R. (1999) Conservation of a gliding motility and cell invasion machinery in Apicomplexan parasites. *J Cell Biol* **147:** 937–944.

Kariu, T., Yuda, M., Yano, K., and Chinzei, Y. (2002) MAEBL is essential for malarial sporozoite infection of the mosquito salivary gland. *J Exp Med* **195:** 1317–1323.

Meis, J.F., Verhave, J.P., Jap, P.H., and Meuwissen, J.H. (1983) An ultrastructural study on the role of Kupffer cells in the process of infection by *Plasmodium berghei* sporozoites in rats. *Parasitology* **86** (Pt 2)**:** 231–242.

Menard, R. (2001) Gliding motility and cell invasion by Apicomplexa: insights from the *Plasmodium* sporozoite. *Cell Microbiol* **3:** 63–73.

Mota, M.M., Pradel, G., Vanderberg, J.P., Hafalla, J.C., Frevert, U., Nussenzweig, R.S., *et al.* (2001) Migration of *Plasmodium* sporozoites through cells before infection. *Science* **291:** 141–144.

Soldati, D., Dubremetz, J.F., and Lebrun, M. (2001) Microneme proteins: structural and functional requirements to promote adhesion and invasion by the apicomplexan parasite *Toxoplasma gondii*. *Int J Parasitol* **31:** 1293–1302.

Spano, F., Putignani, L., Naitza, S., Puri, C., Wright, S., and Crisanti, A. (1998) Molecular cloning and expression analysis of a *Cryptosporidium parvum* gene encoding a new member of the thrombospondin family. *Mol Biochem Parasitol* **92:** 147–162.

Stewart, M.J., and Vanderberg, J.P. (1988) Malaria sporozoites leave behind trails of circumsporozoite protein during gliding motility. *J Protozool* **35:** 389–393.

Sultan, A.A., Thathy, V., Frevert, U., Robson, K.J., Crisanti, A., Nussenzweig, V., *et al.* (1997) TRAP is necessary for gliding motility and infectivity of plasmodium sporozoites. *Cell* **90:** 511–522.

Van Rooijen, N., and Sanders, A. (1994) Liposome mediated depletion of macrophages: mechanism of action, preparation of liposomes and applications. *J Immunol Methods* **174:** 83–93.

Vreden, S.G., Sauerwein, R.W., Verhave, J.P., Van Rooijen, N., Meuwissen, J.H., and Van Den Broek, M.F. (1993) Kupffer cell elimination enhances development of liver schizonts of *Plasmodium berghei* in rats. *Infect Immun* **61:** 1936–1939.

Yuda, M., Sakaida, H., and Chinzei, Y. (1999a) Targeted disruption of the *plasmodium berghei* CTRP gene reveals its essential role in malaria infection of the vector mosquito. *J Exp Med* **190:** 1711–1716.

Yuda, M., Sawai, T., and Chinzei, Y. (1999b) Structure and expression of an adhesive protein-like molecule of mosquito invasive-stage malarial parasite. *J Exp Med* **189:** 1947–1952.

Yuda, M., Yano, K., Tsuboi, T., Torii, M., and Chinzei, Y. (2001) von Willebrand Factor A domain-related protein, a novel microneme protein of the malaria ookinete highly conserved throughout *Plasmodium* parasites. *Mol Biochem Parasitol* **116:** 65–72.

Zieler, H., and Dvorak, J.A. (2000) Invasion *in vitro* of mosquito midgut cells by the malaria parasite proceeds by a conserved mechanism and results in death of the invaded midgut cells. *Proc Natl Acad Sci USA* **97:** 11516–11521.

